Dynamic Contrast-Enhanced CT in Advanced Lung Cancer after Chemotherapy with/without Radiation Therapy: Can It Predict Treatment Responsiveness of the Tumor?

Mi Ri Yoo

Department of Medicine

The Graduate School, Yonsei University

Dynamic Contrast-Enhanced CT in Advanced Lung Cancer after Chemotherapy with/without Radiation Therapy: Can It Predict Treatment Responsiveness of the Tumor?

Mi Ri Yoo

Department of Medicine

The Graduate School, Yonsei University

Dynamic Contrast-Enhanced CT in Advanced Lung Cancer after Chemotherapy with/without Radiation Therapy: Can It Predict Treatment Responsiveness of the Tumor?

Directed by Professor Tae Hoon Kim

The Master's Thesis
submitted to the Department of Medicine
the Graduate School of Yonsei University
in partial fulfillment of the requirements for the degree of Master of Medical Science

Mi Ri Yoo

December 2013

This certifies that the Master's Thesis

of Mi Ri Yoo is approved.

Thesis Supervisor : Tae Hoon Kim

Thesis Committee Member#1 : Young Hoon Ryu

Thesis Committee Member#2 : Yoon Soo Chang

The Graduate School

Yonsei University

December 2013

ACKNOWLEDGEMENTS

I′m distinctly grateful to professor Tae Hoon Kim, thesis supervisor, for his advice and enthusiastic support from planning to the completion of this Master′s thesis, I′m also very grateful to professor Young Hoon Ryu and professor Yoon Soo Chang, thesis committee members for this instructions and feedback which kept me focused in my study.

TABLE OF CONTENTS

LIST OF FIGURES

LIST OF TABLES

ABSTRACT

Dynamic Contrast-Enhanced CT in Advanced Lung Cancer after Chemotherapy with/without Radiation Therapy: Can It Predict Treatment Responsiveness of the Tumor?

Mi Ri Yoo

Department of Medicine
The Graduate School, Yonsei University

(Directed by Professor Tae Hoon Kim)

Purpose: To assess whether the enhancement pattern of tumors at early stages of treatment of advanced lung cancer using a dynamic contrast-enhanced (DCE) CT is an useful tool to predict treatment response during follow-up.

Methods*:* We evaluated two study groups in advanced lung cancer patients who underwent DCE-CT after chemotherapy or chemoradiotherapy. In group A, 65 patients with advanced lung cancer underwent both DCE-CT and PET-CT after the therapy, and the lesions were divided into two groups (noncomplete response and complete response groups) by the maximum standardized uptake value (SUVmax) as 2.5 on the PET-CT images. In group B, 42 patients underwent both DCE-CT and follow-up conventional CT and the lesions were divided into three groups (partial response, stable disease and progressive disease) according to the treatment response evaluated under RECIST 1.1 criteria on follow up conventional CT.

The DCE-CT images were acquired before contrast media injection and 30, 60, 90, 120 seconds, and 5 minute after injection of contrast material. We measured the peak and net enhancement (PE and NE, respectively), relative enhancement ratio (RERs) at each time point, washout (WO) and time-density curves (TDCs) (type A, B, C, and D) on DCE-CT images.

Results*:* The mean PE and NE attenuation values were significantly higher in the noncomplete response (NR) group than in the complete response (CR) group ($p < 0.05$). The DCE-CT images of tumors in the NR group showed rapid enhancement with a sharp acceleration slope, while in the CR group, a slow enhancement pattern was observed until the PE was reached. The RERs till 120 seconds on the DCE-CT images showed moderate correlations with SUVmax on the PET-CT images ($r = 0.373$ to 0.603, $p < 0.05$).

NE and PE values were significantly higher in the progressive disease (PD) group than in the

stable disease (SD) or partial response (PR) groups ($p < 0.05$). Types B, C, and D on TDCs were observed mostly in the PR and SD groups (96.0%), whereas type A was most frequent in the SD and PD groups (97.2%), which were significantly different in terms of PE and NE.

***Conclusions**:* Contrast enhancement patterns on DCE-CT images differed according to treatment results. Therefore, DCE-CT scans can be helpful in predicting treatment response of advanced lung cancer after treatment.

Key Words: Lung cancer, Dynamic Computed Tomography, Treatment Monitoring.

Dynamic Contrast-Enhanced CT in Advanced Lung Cancer after Chemotherapy with/without Radiation Therapy: Can It Predict Treatment Responsiveness of the Tumor?

Mi Ri Yoo

Department of Medicine
The Graduate School, Yonsei University

(Directed by Professor Tae Hoon Kim)

1. INTRODUCTION

Lung cancer continues to increase steadily throughout the world and remains the most common cause of death in cancer patients [1,2]. Patients with unresectable lung cancer are primarily treated with chemotherapy with/without radiation therapy and are regularly followed with computed tomography (CT) scanning to evaluate treatment response [3]. A common method to evaluate treatment response is the Response Evaluation Criteria in Solid Tumor (RECIST) criteria, which depend largely on the longest diameter of the lesion seen on the CT images [4]. It is assumed that the survival of patients who respond according to the RECIST criteria will be prolonged [5]. However, conventional CT may be limited in the assessment of treatment response because the change in tumor size can be insignificant in the early follow-up stages of treatment [6,7].

Non-invasive functional imaging tools are increasingly used in the clinical routines for follow-up evaluation of lung cancers after chemotherapy or radiation therapy. The ^{18}F-fluorodeoxyglucose positron emission tomography (^{18}F-FDG PET), which is based on the higher uptake of ^{18}F-FDG by tumor cells than normal cells, is widely used to evaluate the presence of viable tumor and the growth potential of the tumor [8,9]. Contrast-enhanced magnetic resonance imaging (CE-MRI) can be useful for differentiating between malignant and benign lesions in solitary pulmonary nodules or to monitor treatment response after chemotherapy [10-12]. In recent years, dynamic contrast-enhanced (DCE) CT scanning has been used to differentiate between malignant and benign lesions [13,14]. Only a few studies have used DCE-CT to investigate tumor perfusion or monitor the treatment response of the tumor after chemotherapy or radiation therapy [15,16].

Anatomical changes lag behind functional changes in tumor and responses based on size assessments may become apparent after prolonged treatment duration [612]. Therefore, functional measurement on images is needed.

Our aims in this study were to evaluate the contrast enhancement patterns of lung tumors on the DCE-CT images after chemotherapy with/without radiotherapy and to compare the DCE-CT results with the PET-CT results and finally to assess whether the enhancement pattern of tumors at early stages of treatment can predict treatment response during follow-up.

2. MATERIALS AND METHODS

2.1. Patient selection

Data were collected retrospectively from April 2010 to March 2012 in 165 patients with histologically proven advanced NSCLC (stage III or IV) who were treated chemotherapy with or without radiotherapy. The following patients were excluded from our study: patients who had no residual tumor after treatment, patients who had a residual tumor that was obscured by accompanying pneumonia or post-radiation pneumonitis, patients with poor quality DCE-CT images that prevented accurate assessment of tumor enhancement, and patients who had insufficient renal function (creatinine level > 150 μmol/L) or an allergy to iodinated contrast material. This study was approved by the institutional review board of our hospital (IRB number: 3-2010-0084), and informed consent to use the chest CT and PET-CT images was obtained from all patients.

Of the 165 patients with advanced lung cancer who underwent DCE-CT after chemotherapy with/without radiation therapy, one hundred twenty patients also underwent PET-CT with the time interval of 9 days (interval range, 3 to 14 days). Of 120 patients, 65 (39.4 %) had stable disease based on RECIST according to follow-up CT; these patients were enrolled in group A study. Of the 65 patients, 35 were male, and 30 were female. The mean age at the time of study was 58 years (age range, 34-83 years). A total of 75 lesions in 65 patients were finally selected for analysis. 47 lesions were treated with only chemotherapy, and 28 were treated with chemotherapy and radiation therapy (Table 1).

Of the 165 patients, seventy patients underwent DCE-CT and additional follow-up CT which was performed with a time interval of 3 months. Of 70 patients, 42 patients were enrolled in group B study with rest of them excluded due to the same criteria as above. Of the 42 enrolled patients, 23 were male and 19 were female. The mean age at the time of examination was 66 years (age range, 34-86 years). A total of 61 lesions in 42 patients were finally selected for analysis (Table 1).

2.2 Dynamic contrast-enhanced CT imaging

CT scans were performed with a 64-slice multidetector CT (MDCT) scanner (Somatom Sensation 64; Siemens Medical Solutions, Erlangen, Germany). Scanning was performed in a craniocaudal direction at end-inspiratory suspension with patients in the supine position. After acquiring the scout image to localize the target lesions, we obtained pre-contrast CT images through the target lesions, with the field of view (FOV) as small as possible in order to minimize patients' radiation exposure. After the injection of contrast material, subsequent DCE-CT series were obtained through the lesions at 30, 60, 90, 120 seconds, and 5 minutes. For injection of contrast media, an 18-gauge cannula was placed in the superficial vein of the antecubital fossa. A total of 100 ml of iopromide (Prosure® M300, LG Life Sciences, Seoul, Korea) was administered intravenously at a rate of 4ml/sec using a power injector (Envision CT; Medrad, Pittsburgh, PA) in all patients. The exposure parameters for CT scans were 100 kVp, 175 mA, 1.2 mm collimation, table pitch 1, 500 msec rotation time, 5 mm slice thickness, and a 5 mm reconstruction increment. CT scans at 120 seconds covered the whole thorax with 120 kVp and 175mA for tumor re-staging, which might be changed. The dose-length product (DLP) in the CT units was used to evaluate the radiation dose received by the patient. The effective radiation dose was calculated by multiplying the DLP by the conversion coefficient (k = 0.014) for the chest, and was expressed as millisievert (mSV) [17].

Images were reconstructed on the scanner's workstation using commercially available software (Syngo, Somaris 5®; Siemens Medical Solutions, Germany), with a slice thickness of 5 mm by using a standard algorithm. All dynamic and staging CT data were transferred to our picture archiving and communication system (PACS) (Centricity 1.0; GE Medical Systems, Mt Prospect, Ill), which displayed all images on monitors (1536 x 2048 image matrices, 60-foot-lambert luminescence).

Table 1. Patient characteristics, treatment methods and histologic findings of the two groups.

Group A: DCE-CT with PET-CT		**Group B: DCE-CT with follow up conventional CT**	
Characteristics	Value	Characteristics	Value
Age	year	Age	year
Mean	60	Mean	66
Range	34-83	Range	34-86
Sex	n=65	Sex	n=42
Man	35	Man	23
Woman	30	Woman	19
Histologic finding	n=75	Histologic finding	n=61
Adenocarcinoma	51	Adenocarcinoma	32
Squamous cell carcinoma	23	Squamous cell carcinoma	19
NSCLC, NOS*	1	NSCLC, NOS*	10
Treatment methods		Treatment methods	
Chemotherapy only	47	Chemotherapy only	46
Chemoradiotherapy	28	Chemoradiotherapy	15
Chemotherapy agent		Chemotherapy agent	
Cisplatin based doublet†	45	Cisplatin based doublet†	29
EGFR tyrosine kinase inhibitor‡	18	EGFR tyrosine kinase inhibitor‡	17
Single agent§	12	Single agent§	15

Note. Except for age and sex, values are number of the lesions. NSCLC = non-small cell lung cancer, EGFR = epidermal growth factor receptor, NOS = not otherwise specified.

*Confirmed as NSCLC with needle aspiration biopsy but not categorized into any of the subtype of NSCLC on pathologic report.

†Cisplatin with gemcitabine, docetaxel, paclitaxel, pemetrexel or irinotecan.

‡Erlotinib or gefinitib

§Non-cisplatin single agent such as gemcitabine, docetaxel, pemetrexed.

2.3 DCE-CT image analysis

Images were evaluated by consensus of two radiologists who had 4 and 20 years of experience

in interpreting chest images, respectively, in one image interpretation session. All images were set at a window width of 400 Hounsfield units (HU) and a window level of 20 HU to measure the attenuation values of the lesions on the serial dynamic CT images. Tumor attenuation values (TAV_t, in HU) of the targeted lesions, where t indicates each designated time point before and after the injection of contrast material on the serial dynamic CT images, were measured. A circular region of interest (ROI) [18] as large as possible was drawn within the lesions, and necrotic areas, cavities, and calcifications were avoided. We avoided lesion with more than 100 HU to exclude adjacent atelectatic lung parenchyma and we targeted only tumor surrounded by normal aerated lung parenchyma that is not adjacent to the consolidation or fibrosis. Mean values were calculated based on two measurements obtained from two ROIs in each lesion form the dynamic series of images. The size of the tumor was measured by the longest diameter of the lesions on the images taken at 90 seconds after the injection of contrast material.

We then analyzed the peak enhancement (PE), the time it took to reach the PE, the net enhancement (NE), the relative enhancement ratio (RER_t, in %) at each designed time point, and the washout (WO) after the PE was reached of all targeted lesions. The RER_t of the lesions was assessed using the following equation: RER_t (%) = $[(TAV_t - TAV_0)/TAV_0] \times 100$, where TAV_0 was the attenuation value on the pre-contrast images. PE was defined as the first maximum attenuation value at the designated time (TAV_t) during the dynamic period after the injection of contrast material. The NE value was calculated as ($PE - TAV_0$). The WO value of the lesion was calculated as ($PE - TAV_{300}$) [14].

The DLP in the CT units was used to evaluate the radiation dose received by the patient. The effective radiation dose was calculated by multiplying the DLP by the conversion coefficient ($k = 0.014$) for the chest, and was expressed as millisievert (mSV).

2.4. ^{18}F-fluorodeoxyglucose PET-CT examination

PET-CT scans were performed using a whole-body tomography scanner (Biograph40; Siemens Medical Solutions, Chicago, Illinois, USA). This scanner provides a 16.2 cm axial field of view (FOV) and a 60.5 cm transaxial FOV, resulting in 81 image planes spaced 2-mm apart. The transaxial spatial resolution was 4.2-mm full-width at half-maximum at the center of the FOV, and the axial resolution was 4.7 mm full-width at half-maximum.

Patients fasted for at least 6 hours and maintained a blood glucose level of below 140 mg/dl before intravenous injection of 370 MBq (10mCi) ^{18}F-FDG. All patients were studied in the supine position with their arms raised. The PET emission scan was performed immediately after CT scanning without changing the patient's position. Whole-body emission images were obtained 60 minute after injection of radioisotope in all patients using the multiple-bed position

technique. Six to seven bed positions from the base of the skull to the upper thigh were imaged for 2 minute per bed position. Additional images were then acquired for brain evaluation. The PET images were reconstructed with an iterative transmission algorithm in the transaxial, coronal, and sagittal planes. The CT data were corrected for attenuation, and image fusion of PET and CT images was performed on the navigator and wizard workstation using commercially available imaging software (Syngo, Siemens Healthcare, Forchheim, Germany).

2.5. ^{18}F-fluorodeoxyglucose PET-CT analysis

To measure the standardized uptake values (SUV) of lesions, an attending radiologist board-certified in radiology and nuclear medicine with 20 years' experience in oncologic imaging reviewed the PET-CT images on the workstation and drew ROIs over the targeted lesions. Tumors were evaluated by measuring the maximum SUV (SUVmax) on the PET-CT images. The SUVmax was defined as the highest SUV among all voxels within the ROI drawn on the targeted lesion. All 65 residual tumors on the CT images were divided into two groups according to the SUVmax on the PET-CT images: a complete response (CR) group that comprised residual tumors that had an SUVmax less than 2.5, and a non-complete response (NR) group that had residual tumors with an SUVmax equal to or greater than 2.5 [19].

2.6. Time density curve (TDC) analysis

In order to analyze the enhancement pattern on the dynamic CT images, we plotted the mean attenuation values of the lesions at each time point as a time-density curve (TDC). TDCs were classified as one of the following four types according to wash-in and wash-out patterns: type A, an early wash-in and early wash-out pattern; type B, an early wash-in and maintaining a plateau; type C, an early wash-in and then continuous acceleration during the dynamic period; and type D, net enhancement less than 15 HU without an early wash-in pattern during the dynamic period.

2.7 Evaluation of treatment response

On follow-up CT scans, the treatment response was evaluated according to the RECIST criteria (RECIST 1.1) as follows: complete response (CR), disappearance of lesions; partial response (PR), at least a 30% decrease in the diameter of the lesion on the follow-up CT images; progressive disease (PD), a more than 20% and 5 mm absolute increase in lesion diameter; stable disease (SD), neither sufficient shrinkage of the lesion to qualify for PR nor a sufficient increases in size to qualify for PD [4]. In this study, these treatment response evaluations are only targeted on the measurable lesion in the lung parenchyma regardless of other lesions including

lymph node, metastatic lesion.

2.8 Statistical Analysis

In group A, we used Student's t test to evaluate the statistical significance of differences in PE, time to reach PE, NE, RERt and WO of the selected tumors in the CR and the NR groups. Pearson correlation was used to evaluate relationships between PE, NE, RERt and WO on DCE-CT images and SUVmax on PET-CT images of the target lesions. Receiver operating characteristic (ROC) curves were used to determine the diagnostic performance and cutoff values of contrast enhancements by DCE-CT after chemotherapy with/without radiation therapy that were consistent with a CR. The discriminatory property of each significant index on DCE-CT images was assessed by calculating areas under the curve (AUCs) with an associated confidence interval of 95 %. Multivariate analysis consisted of logistic regression analysis for independent CT measurements related to NR tumor.

And in group B, Fisher's exact test was used to evaluate differences of distribution of three groups formed based on the RECIST criteria between TDC type A and type B, C, D. And then, we used an analysis of variance (ANOVA) to evaluate the statistical significance of differences in PE and NE values among the three groups in lesions with type A TDC pattern. ROC analysis was performed to evaluate cutoff values of WI and WO to predict the treatment response.

A p value less than 0.05 was considered to be significant. Calculations were performed with SPSS software (version 17.0; the Statistical Package for the Social Sciences, Chicago, IL). All parameters are reported as means ± standard deviations.

3. RESULTS

3.1 In group A

The tumor characteristics of the 75 lesions in 65 patients are summarized in Table 1. The mean effective radiation dose for the dynamic CT scans in 65 patients was 3.3 mSV (dose range, 2.9-5.2 mSV). Of the patients, 26 (40%) were assigned to the CR group and 39 (60%) to the NR group according to the SUVmax values. The mean SUVmax was 1.6 ± 0.4 in the CR group and 8.4 ± 3.8 in the NR group. The mean tumor size in the NR group (4.1 ± 1.9 cm) was significantly larger than that in the CR group (2.9 ± 1.7 cm; $p < 0.01$). The mean PE and NE values were significantly higher in the NR group (72.1 ± 10.7 HU and 37.8 ± 9.8 HU, respectively) than in the CR group (61.5 ± 12.4 HU and 25.4 ± 12.1 HU, respectively) ($p < 0.05$). Although the time to reach PE was shorter in the NR group (105.4 ± 43.7 sec) than in the CR group (122.0 ± 54.9 sec), this difference was not statistically significant ($p > 0.05$). The RERs were much higher in the NR group than in the CR group at all-time points after the

injection of contrast material except at 5 minute ($p < 0.05$). The WO was also higher in the NR group (11.4 ± 9.1 HU) than in the CR group (4.9 ± 8.0 HU) ($p < 0.05$) (Table 2).

Table 2. Tumor characteristics for 75 lesions on DCE-CT images according to the SUVmax in 65 patients with advanced NSCLC

Tumor Characteristics	CR (n = 28)	NR (n = 47)	*p* value[a]
SUVmax	1.6±0.4	8.4±3.8	
Tumor size (cm)	2.9±1.7	4.1±1.9	< 0.05
PE (HU)	61.5±12.4	72.1±10.7	< 0.05
NE (HU)	25.4±12.1	37.8±9.8	< 0.05
Time-PE (s)	122.0±54.9	105.4±43.7	> 0.05
UnAV (HU)	36.0±6.2	34.3±4.0	
RER (%)			
at 30 s	23.8±28.3	65.6±36.7	< 0.05
at 60 s	34.3±34.8	99.2±32.1	< 0.05
at 90 s	55.4 ± 38.1	99.7 ± 23.5	< 0.05
at 120 s	71.0 ± 38.7	103.7 ± 37.1	< 0.05
at 300 s	59.4 ± 32.0	78.6 ± 32.9	> 0.05
WO (HU)	4.9 ± 8.0	11.4 ± 9.1	< 0.05

Note. *SUVmax* maximum standardized uptake value, *PE* peak enhancement, *NE* net enhancement, *Time-PE* time to reach peak enhancement, *HU* Hounsfield unit, *UnAV* unenhanced attenuation value, *RER* relative enhancement ratio, *WO* washout value, *CR* and *NR* complete metabolic and non-complete metabolic response groups according to SUVmax

[a] *p* values were determined using Student's *t* test

The mean tumor attenuation values on the DCE-CT images for the two groups are shown in Figure 1. NR group tumors showed a rapid enhancement pattern with a sharp acceleration slope (Figure 1 and 2), whereas in the CR group, the residual tumors had a slow enhancement pattern until peak enhancement (Figure 1 and 3). Attenuation values and RERs obtained by DCE-CT for the 75 lesions showed moderate correlation with SUVmax measured by PET-CT (r = 0.373 to 0.604). However, there were no correlations in the enhancement values at 5 minute and the WO between DCE-CT and PET-CT ($p > 0.05$) (Table 3)

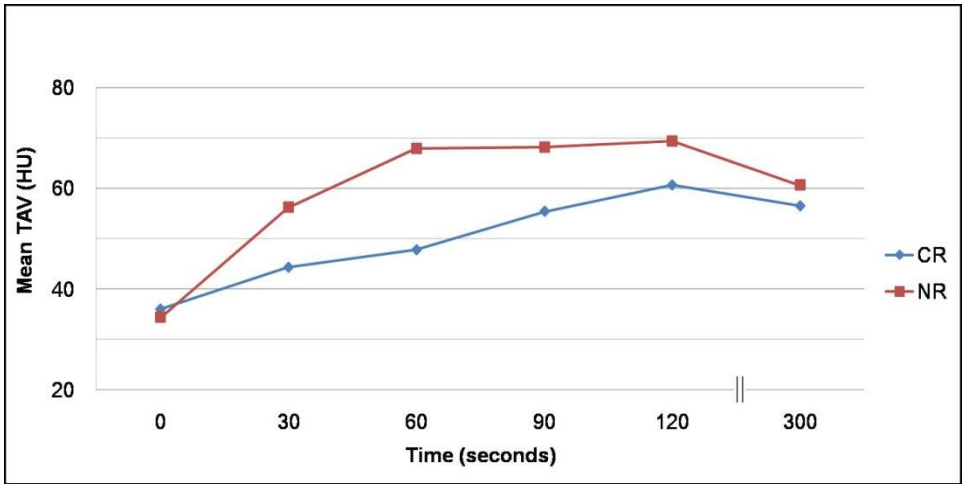

Figure 1 Mean attenuation values in Hounsfield units of tumors on DCE-CT images according to SUVmax on PET-CT images. The NR group had a steeper contrast enhancement curve slope and near peak enhancement was reached earlier (60 s) than the CR group. Attenuation value reached a peak value at 120 s. Serial dynamic CT images from the NR group showed a slow enhancement pattern until peak enhancement was reached. TAV at each corresponding time is represented with mean ± standard deviation

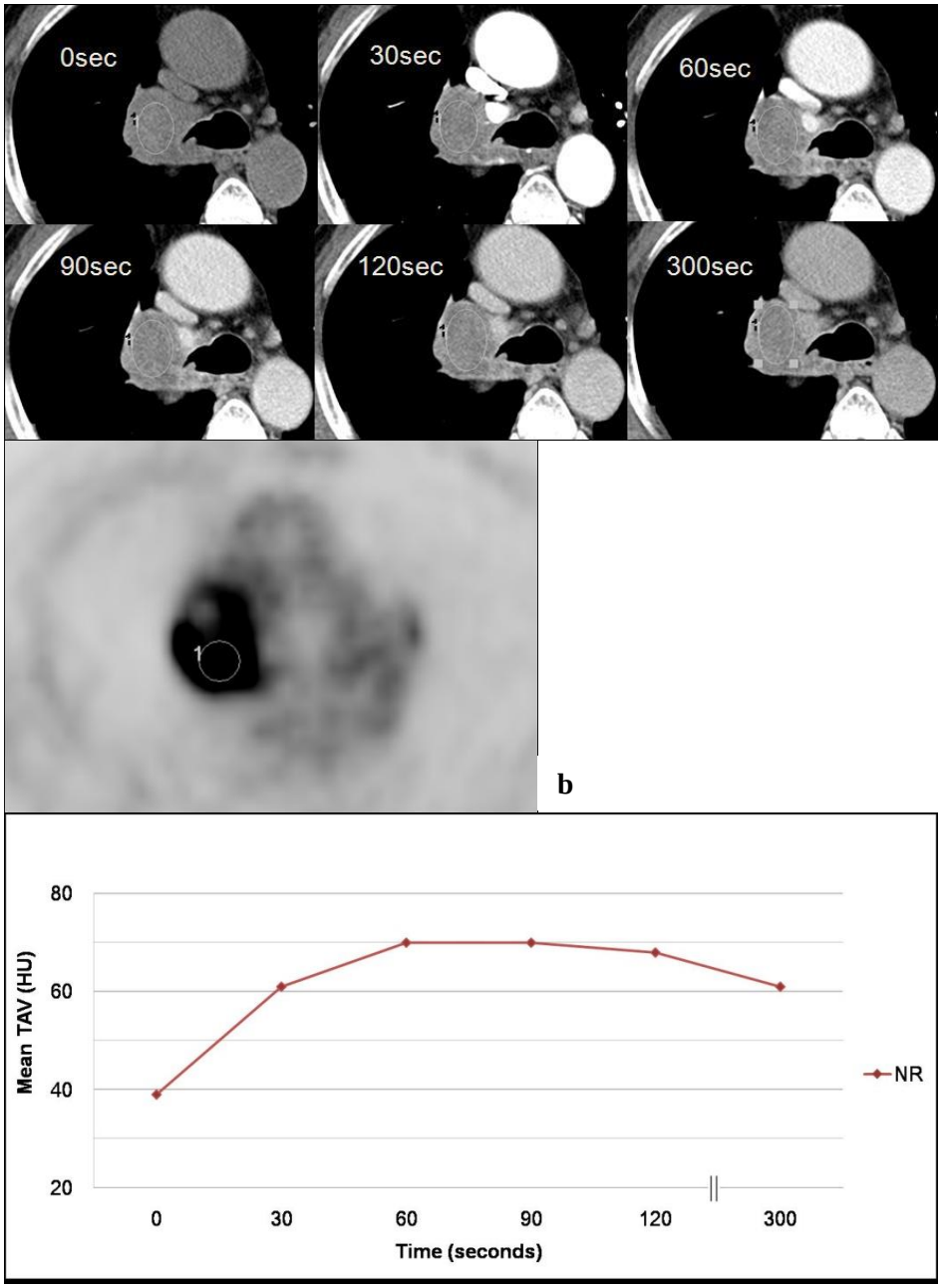

Figure 2 Imaging study of NR group according to SUVmax on PET-CT images. A 63-year-old male patient with adenocarcinoma in the right upper lobe treated by chemotherapy. **a.** Attenuation values of the lesion on serial dynamic CT images were obtained precontrast and at 30, 60, 90, 120 s and 5 min after contrast material injection. The longest tumor diameter was 4.1 cm. **b.** The SUVmax by PET image was 8.3. **c.** The time–attenuation curve showed the NR pattern. PE and NE values were 70 and 33 HU. *TAV* tumor attenuation value, *HU* Hounsfield units

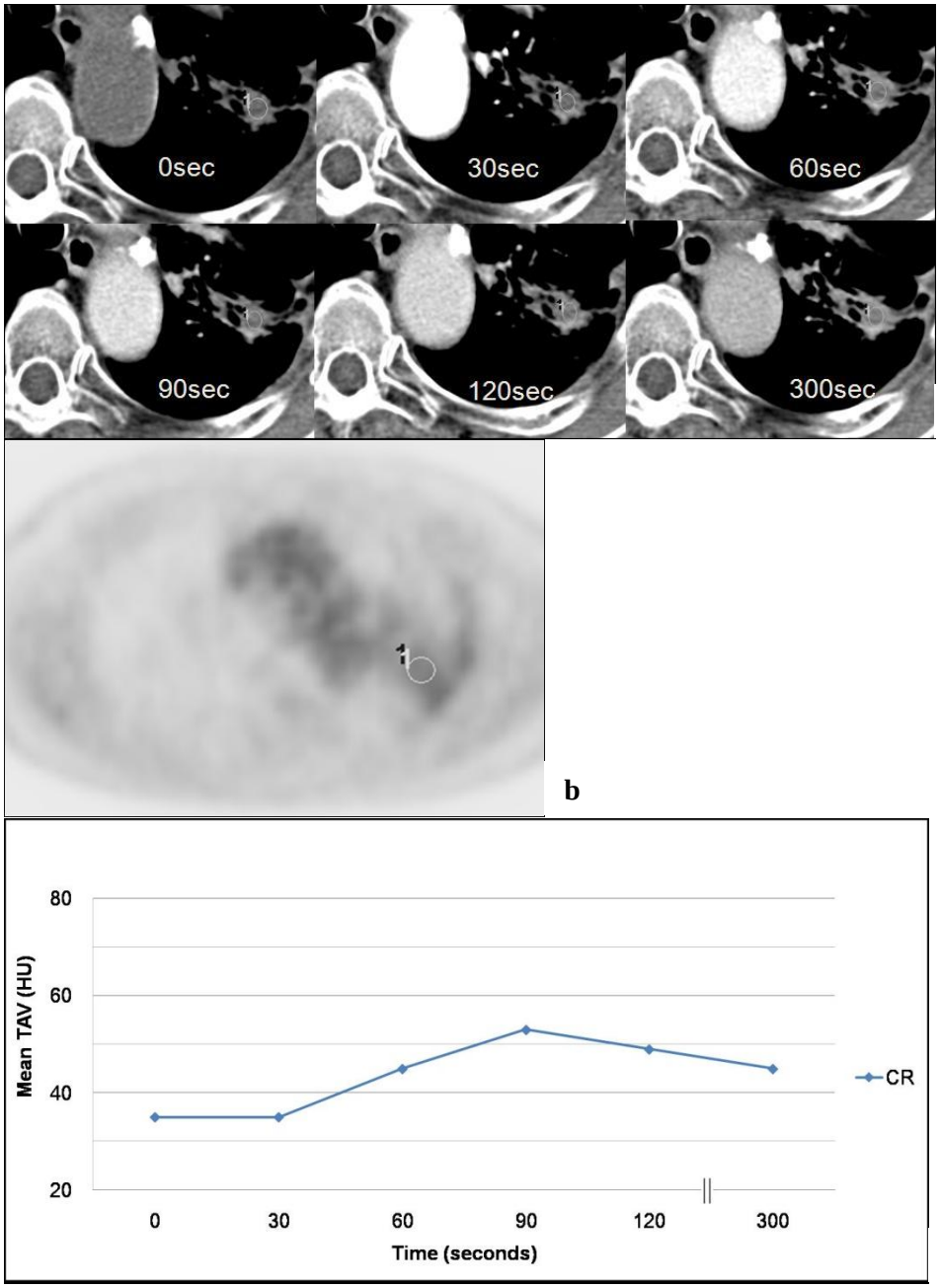

Figure 3 Imaging study of CR group according to SUVmax on PET-CT images. A 57-year-old female patient with adenocarcinoma in the left upper lobe treated by chemotherapy and radiation therapy. **a.** Attenuation values of the lesion on serial dynamic CT images were obtained unenhanced and at 30, 60, 90, 120 s and 5 min after contrast material injection. The longest tumor diameter was 1.5 cm. **b.** The SUVmax on PET image was 0.8. **c.** Time–attenuation curve showed the CR pattern. The PE and NE values were 57 and 27 HU. *TAV* tumor attenuation value, *HU* Hounsfield units

Table 3. Relationships between tumor measurement from DCE-CT images and SUVmax from PET-CT images for 75 lesions after treatment

DCE-CT measurements	r value for SUVmax	*p* value
Tumor size (cm)	0.566	<0.05
PE (HU)	0.410	< 0.05
NE (HU)	0.461	< 0.05
RER (%)		
at 30 sec	0.418	< 0.05
at 60 sec	0.604	< 0.05
at 90 sec	0.503	< 0.05
at 120 sec	0.373	< 0.05
at 300 sec	0.285	> 0.05
WO (HU)	0.263	> 0.05

Note. *DCE-CT* = dynamic contrast-enhanced CT, *SUVmax* = maximum standardized uptake value, *PET-CT* positron emission tomography CT, *PE* peak enhancement, *NE* net enhancement, *HU* Hounsfield Unit, *RER* relative enhancement ratio, and *WO* wash-out value. Correlation coefficients and *p* values were determined by a Pearson correlation.

The AUC for each enhancement index on DCE-CT are in Table 4. RER_{60} showed the largest AUC (0.90) under the 95% confidence interval (CI; 0.81 - 0.98, $p < 0.01$) (Fig. 4). When the optimal RER_{60} cutoff point was set at 43.7% to differentiate between the CR and NR groups, sensitivity was 95.7 %, specificity was 64.2 %, positive predictive value was 82.1 % and negative predictive value was 95.0 %. Diagnostic accuracy was 88.8 %. After adjusting for tumor size, the odd ratio for NR in tumors with an RER60 of at least 43.7 % was 70.85 (95 % CI = 7.95–630.91; $p < 0.05$) (Table 5).

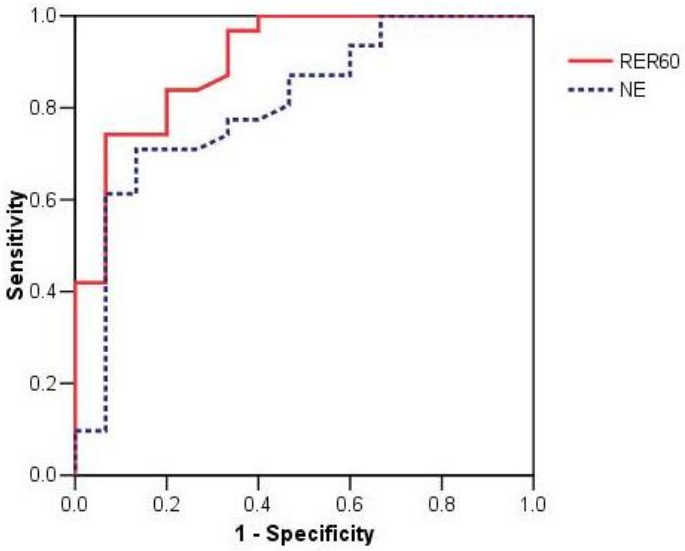

Figure 4 ROC curves based on the RER_{60} and NE measured from DCE-CT images

Table 4. ROC curve analysis of tumor measurements from DCE-CT images for 75 lesions after treatment

DCE-CT measurements	AUC	*p* value
Tumor size (cm)	0.80	<0.05
PE (HU)	0.78	< 0.05
NE (HU)	0.80	< 0.05
RER (%)		
at 30 sec	0.82	< 0.05
at 60 sec	0.90	< 0.05
at 90 sec	0.83	< 0.05
at 120 sec	0.72	< 0.05
at 300 sec	0.66	> 0.05
WO (HU)	0.79	< 0.05

Note. *The ROC curve* the Receiver Operating Characteristic curve, *DCE-CT* dynamic contrast-enhanced CT, *AUC* the area under the curve, *PE* peak enhancement, *NE* net enhancement, *HU* Hounsfield unit, *RER* relative enhancement ratio, and *WO* wash-out value.

Table 5. Multivariable logistic regression analysis of DCE-CT measurements related to NR of tumor after treatment

DCE-CT measurements	Odds ratio	95 % CI	*p* value
S2 (>3 cm and ≤5 cm)	1.59	0.30–8.24	>0.05
S3 (>5 cm)	1.47	0.30–7.20	>0.05
$RER_{60} \geq 43.7$ %	70.85	7.95–630.91	<0.05

Note. RER_{60} relative enhancement ratio at 60 seconds after contrast media injection, and *CI* confidence interval. Independent CT measurements related to NR group were determined by multivariate analysis consisted of logistic regression analysis.

3.2 In group B

The tumor characteristics of the 61 lesions in 42 patients are summarized in Table 1. The mean effective radiation dose for the dynamic CTs studies in 42 patients was 3.5 mSV (dose range, 2.9–5.4 mSV). The radiation dose for the chest CTs examinations ranged from 2.4 to 5.8 mSV. On the basis of treatment response assessed by the RECIST criteria, there were 7 PR lesions (11.5%), 16 PD lesions (26.2%), and 38 SD lesions (62.3%). The mean longest diameter of all tumors was 2.9 ± 1.7cm (range, 0.9 to 8.6 cm); 2.8 ± 1.0 cm in PR, 3.2 ± 2.0 cm in SD, and 2.2 ± 0.8 cm in PD. The mean NE values were 46.5 ± 14.9 HU in PR, 44.9 ± 18.2 HU in SD, and 63.1 ± 13.5 HU in PD group, respectively. The PE mean values were 83± 14.9 HU in PR, 81.9 ± 18.3 HU in SD, and 98.4 ± 12.5 HU in PD group, respectively (Table 6). No matter radiation therapy was combined or not, kind of chemotherapy agent, enhancement pattern was not changed statistically ($p < 0.05$).

Table 6. Tumor size and degree of contrast enhancement according to the RECIST classification

RECIST	Diameter (cm)	NE (HU)	PE (HU)
PR (n = 7)	2.8 ± 1.0	46.5 ± 14.9	83.0 ± 14.9
SD (n = 38)	3.2 ± 2.0	44.9 ± 18.2	81.9 ± 18.3
PD (n = 16)	2.2 ± 0.8	63.1 ± 13.5	98.4 ± 12.5
p value		< 0.05	< 0.05

Note. *PR* partial response, *SD* stable disease, *PD* progressive disease, *NE* net enhancement, *PE* peak enhancement. Difference in diameter, PE and NE values among the three groups were determined by analysis of variance (ANOVA). Data are mean ± standard deviations.

The TDCs showed that there were 36 type A lesions (Fig. 6), 7 type B, 16 type C (Fig. 7), and 2 type D lesions. There was statistically significant difference of distribution of RECIST groups between the type A lesions and the other types of groups ($p < 0.05$). Most lesions that were type B (100%), type C (93.8%), or type D (100%) on the TDCs belonged to the PR and SD groups according to the RECIST criteria. There were 35 lesions showing a type A pattern on the TDCs that belonged to the SD or PD groups. The SD group comprised 20 (55.6%) and the PD group included 15 lesions (41.7%) (Table 7).

The mean values of NE and PE were significantly higher in the PD group than in the PR or SD groups according to the RECIST criteria (Fig. 5) ($p < 0.05$). The ROC curve analysis of NE values indicated that the sensitivity and specificity were 62.5% and 82.2%, respectively, with a NE value of 60.3 HU as a cutoff value to differentiate between the PD group and the PR or SD groups. When the cutoff value was set at 94.5 HU for the PE value, the sensitivity and specificity were 75.0% and 75.6%, respectively (Fig. 8). Therefore, with using these cutoff values, the SD or PD groups both showing the type A TDC pattern can be differentiated.

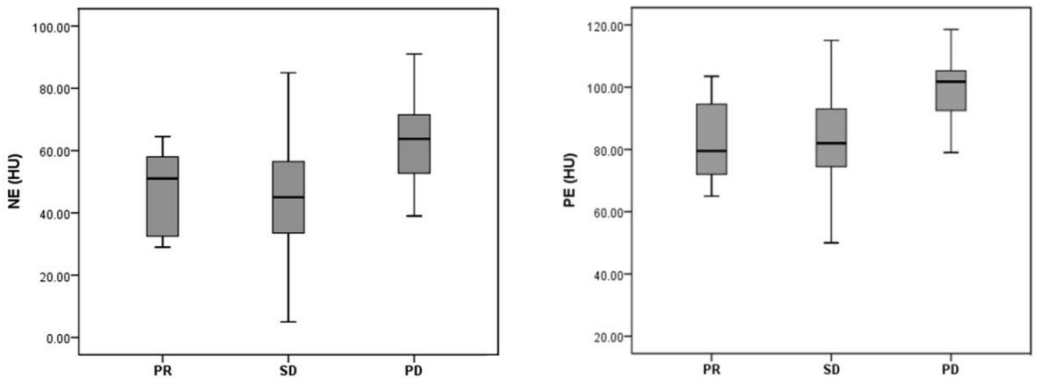

a **b**

Figure 5. Mean values of NE and PE in 61 lesions among three groups according to the RECIST criteria in 41 patients with advanced lung cancer. **a.** NE differed significantly between the PD group and the PR or SD groups ($p < 0.05$). **b.** PE differed significantly between the PD group and the PR or SD groups ($p < 0.05$). *PR* partial response, *SD* stable disease, and *PD* progressive disease. Difference in PE and NE values between the PD group and the PR or SD groups were determined by analysis of variance (ANOVA).

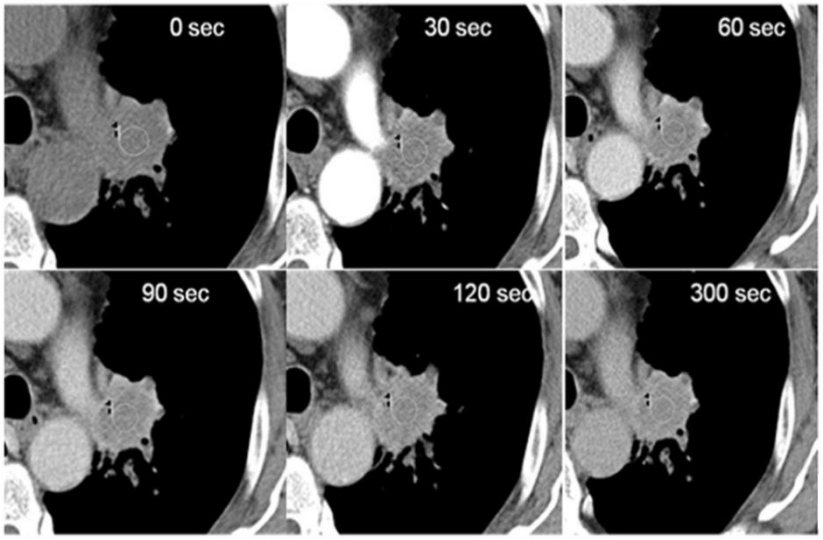

a

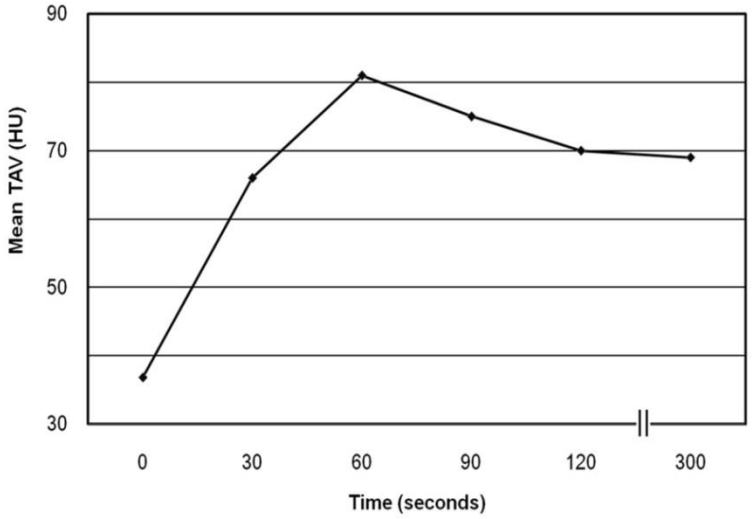

b

Figure 6. Imaging study of type A TDC pattern on DCE-CT images. A 69-year-old man with stage IV non-small cell carcinoma in the left upper lobe with lung to lung metastasis. **a.** DCE-CT images at pre-contrast, 30, 60, 90, 120 sec, and 5 minutes over the lesion after chemotherapy with a cisplatin regimen. **b.** TDC shows early wash-in and wash-out pattern consistent with type A. NE and PE values were 44 HU and 81 HU, respectively. The lesion was categorized as progressive disease according to the RECIST criteria. *TAV* tumor attenuation value.

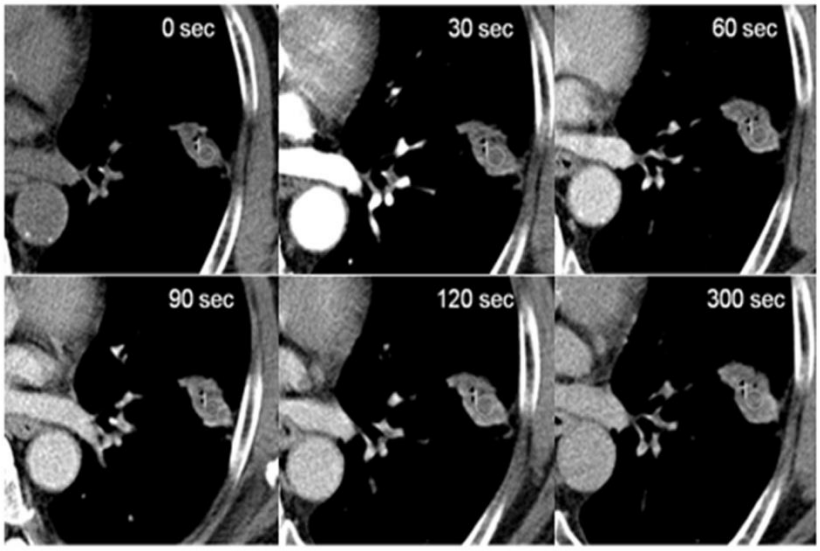

a

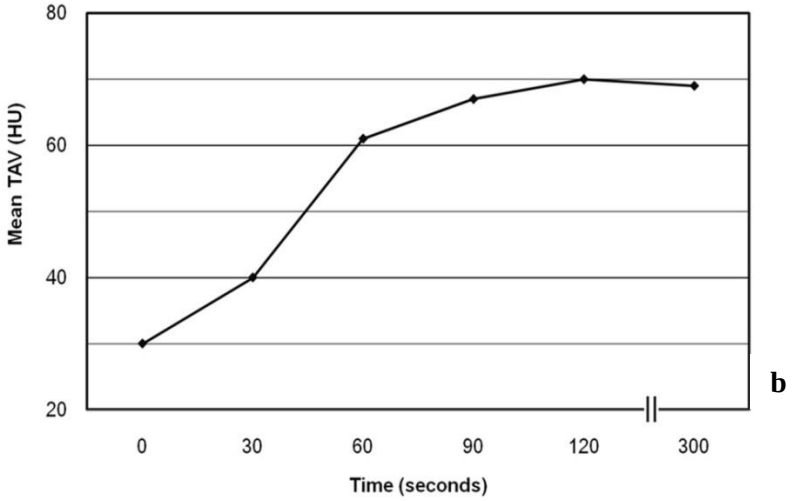

b

Figure 7. Imaging study of type C TDC pattern on DCE-CT images. A 83-year-old woman with stage IV adenocarcinoma in the left upper lobe. **a.** DCE-CT images at pre-contrast, 30, 60, 90, 120 sec, and 5 minutes over the lesion after chemotherapy with a Gefinitib regimen. **b.** The TDC shows early wash-in and continuous acceleration pattern consistent with type C. NE and PE values were 40 HU and 70 HU, respectively. The lesion was categorized as SD according to the RECIST criteria. *TAV* tumor attenuation value.

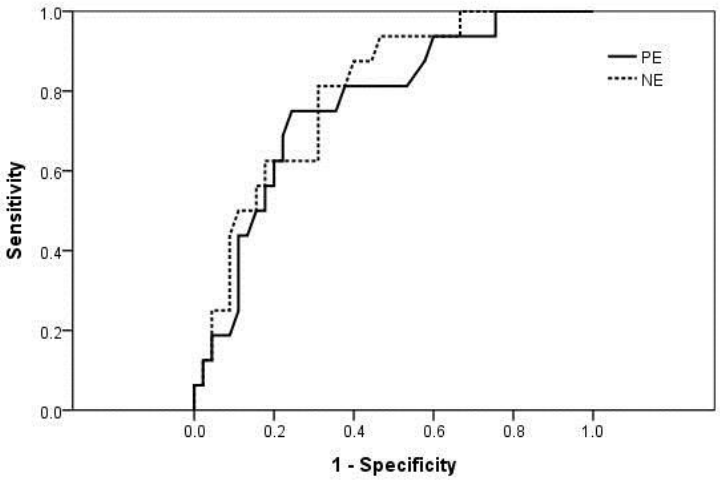

Figure 8. ROC curves of PE and NE values. Sensitivity and specificity for differentiating between the PD group and the PR or SD groups were 62.5% and 82.2%, respectively, at a cutoff NE value of 60.3 HU, and 75.0% and 75.6%, respectively, at a cutoff PE value of 94.5 HU. *PR* partial response, *SD* stable disease, and *PD* progressive disease.

Table 7. TDC according to the RECIST groups

RECIST	Types of Time-Density Curve (TDC)*				Total (n)
	A	B	C	D	
PR	1	3	3	0	7
SD	20	4	12	2	38
PD	15	0	1	0	16
Total (n)	36	7	16	2	61

Note. *PR* = partial response, *SD* = stable disease, *PD* = progressive disease, *A showing an early WI and early WO, B showing an early WI and maintaining a plateau, C showing an early WI and continuous acceleration, and D showing no early WI in the dynamic period. Fisher's exact test was used to evaluate differences of three groups formed based on the RECIST criteria between type A and type B, C, D.

4. DISCUSSION

It is clinically important for imaging studies to noninvasively monitor treatment response during the follow up period after chemotherapy with/without radiation therapy. However, it is difficult to evaluate treatment response in the early follow-up stages of treatment because the change in lesion size may be insignificant according to the RECIST criteria [6,12].

Only a few studies reported that the dynamic contrast enhancement pattern could be useful in assessing the blood supply in tumor tissue and in predicting treatment outcomes [12,20]. Lind et al. [15] reported that blood flow into the tumor decreased more significantly in the RECIST/Crabb responders rather than in the non-responders and was negatively correlated with progression free survival. Donmez et al. [21] demonstrated most of the malignant lesions had early peak enhancement with rapid washout on dynamic MRI.

Enhancement of contrast material on the DCE-CT images has mostly been used to differentiate between tumors with benign and malignant characteristics, especially lung cancers [13,14,22]. A wide range of maximum attenuation values (from 20 to around 60 HU) has been reported to be a good predictor of lung malignancy based on incremental dynamic CT [23]. Yi et al. [13] reported that a cutoff NE value of 30 HU or more showed good sensitivity for differentiating between benign and malignant lesions on the DCE-CT images. These authors also showed that malignant lesions had high NE and PE values because of their high microvessel density. And these malignant lesions had a steeper enhancement slope on the early acceleration phase on the DCE-CT images [13]. However, this type of enhancement pattern is usually reported for pre-treatment tumors. Treatment with a chemotherapy with/without radiation therapy can potentially change the microvessel density of tumors and therefore the extent of enhancement on the contrast-enhanced CT images [24].

Although we examined malignant lesions after chemotherapy with/without radiation therapy, the DCE-CT images of lesions with SUVmax $\geq$ 2.5 (NR group) showed rapid enhancement with a sharp acceleration slope compared with the slow enhancement pattern observed in images of lesions with SUVmax < 2.5 (CR group). These findings suggest that residual tumors with a high SUVmax still have high microvessel density after treatment. And the mean PE and NE values were significantly higher in the NR group than in the CR group and in the PD group than in the PR and SD groups. In the group B of our study, significantly high PE and NE values were observed in PD group and most of the type A lesions which shows early WI and WO pattern on dynamic CT were included in SD and PD groups on the follow up conventional CT which can be differentiated with PE and NE values.

FDG-PET scanning provides information about glucose metabolism in the tumors and can help predict patient survival after chemotherapy or radiation therapy. The prognosis of patients with positive FDG-PET tumors was worse than that of patients who had negative results, and an SUVmax cutoff value of 2.5 was suggested to differentiate tumors with a CR from those with a NR after three cycles of neoadjuvant chemotherapy [25,26]. Although we did not evaluate the survival of patients after treatment, patients who had a high SUVmax on FDG-PET images showed an enhancement pattern characteristic of malignant lesions on the DCE-CT images.

Generally, the tumor response to radiation therapy is believed to be slow in process with maximum response (minimum volume), an average of 5–11 months after radiation therapy completion [2728]. 28 lesions and 15 lesions were treated with chemoradiotherapy in the first and second study groups with mean interval between termination of radiotherapy and time of dynamic CT taken were 292 days (range, 86 to 600 days), which might be explained that radiation itself may little effect on acute microvascular damage. And whether radiation therapy was combined or not, enhancement pattern was not affected statistically ($p > 0.05$). Also 61 lesions with chemotherapy showed no significant difference of enhancement pattern according to the chemotherapy agent whether cytotoxic or cytostatic agent ($p > 0.05$)

Our study has some limitations that will be overcome in the future. First, the study population was too small to generalize the result. And, neither the viability of tumors after chemotherapy or chemoradiotherapy treatment nor the microvessel density was confirmed histologically. Third, we did not evaluate the relationship between the enhancement pattern on the DCE-CT images and the survival rate of the patients after the treatment. Fourth, we did not directly compare the enhancement pattern of the targeted lesions on the DCE-CT images or the SUVmax on the FDG-PET images between before and after treatment. Finally, manual ROI measurement can be subjective due to variable enhancement in the tumor and small remained size after exclusion of necrosis and cavity in the tumor. Also SUVmax can be subjective compare to SUVmean.

5. CONCLUSION

The enhancement pattern of lesions on the DCE-CT images that showed NR on FDG-PET images was similar to that of malignant lesions before treatment. The mean PE and NE values were significantly higher in the NR group than in the CR group, and the DCE-CT images of NR tumors show rapid enhancement with a sharp acceleration slope, where the DCE-CT images of CR tumors showed a slow enhancement pattern until the PE was reached. In the same manner, it shows similar results as assessed with RECIST criteria, in that the SD and PD groups showing type A TDC pattern of contrast enhancement can be differentiated according to PE or NE values, significantly higher in the PD group than the SD or PR groups. Therefore, the enhancement pattern of tumors on the DCE-CT images can potentially be used to evaluate the status of these tumors after chemotherapy with/without the radiation therapy in patients with advanced lung cancer.

References

1. Jemal A, Siegel R, Ward E, Murray T, Xu J, Thun MJ. Cancer statistics, 2007. CA Cancer J Clin 2007;57:43-66.

2. Schiller JH, Harrington D, Belani CP, et al. Comparison of four chemotherapy regimens for advanced non-small-cell lung cancer. N Engl J Med 2002;346:92-8.

3. Pfister DG, Johnson DH, Azzoli CG, et al. American Society of Clinical Oncology treatment of unresectable non-small-cell lung cancer guideline: update 2003. Journal of clinical oncology : official journal of the American Society of Clinical Oncology 2004;22:330-53.

4. Eisenhauer EA, Therasse P, Bogaerts J, et al. New response evaluation criteria in solid tumours: revised RECIST guideline (version 1.1). Eur J Cancer 2009;45:228-47.

5. Lara PN, Jr., Redman MW, Kelly K, et al. Disease control rate at 8 weeks predicts clinical benefit in advanced non-small-cell lung cancer: results from Southwest Oncology Group randomized trials. Journal of clinical oncology : official journal of the American Society of Clinical Oncology 2008;26:463-7.

6. Suzuki C, Jacobsson H, Hatschek T, et al. Radiologic measurements of tumor response to treatment: practical approaches and limitations. Radiographics 2008;28:329-44.

7. Mazumdar M, Smith A, Schwartz LH. A statistical simulation study finds discordance between WHO criteria and RECIST guideline. J Clin Epidemiol 2004;57:358-65.

8. Dorow DS, Cullinane C, Conus N, et al. Multi-tracer small animal PET imaging of the tumour response to the novel pan-Erb-B inhibitor CI-1033. Eur J Nucl Med Mol Imaging 2006;33:441-52.

9. Su H, Bodenstein C, Dumont RA, et al. Monitoring tumor glucose utilization by positron emission tomography for the prediction of treatment response to epidermal growth factor receptor kinase inhibitors. Clin Cancer Res 2006;12:5659-67.

10. Schaefer JF, Vollmar J, Schick F, et al. Solitary pulmonary nodules: dynamic contrast-enhanced MR imaging--perfusion differences in malignant and benign lesions. Radiology 2004;232:544-53.

11. Zou Y, Zhang M, Wang Q, Shang D, Wang L, Yu G. Quantitative investigation of solitary pulmonary nodules: dynamic contrast-enhanced MRI and histopathologic analysis. AJR Am J Roentgenol 2008;191:252-9.

12. de Langen AJ, van den Boogaart V, Lubberink M, et al. Monitoring response to antiangiogenic therapy in non-small cell lung cancer using imaging markers derived from PET and dynamic contrast-enhanced MRI. J Nucl Med 2011;52:48-55.

13. Yi CA, Lee KS, Kim EA, et al. Solitary pulmonary nodules: dynamic enhanced multi-detector row CT study and comparison with vascular endothelial growth factor and microvessel

density. Radiology 2004;233:191-9.

14. Jeong YJ, Lee KS, Jeong SY, et al. Solitary pulmonary nodule: characterization with combined wash-in and washout features at dynamic multi-detector row CT. Radiology 2005;237:675-83.

15. Lind JS, Meijerink MR, Dingemans AM, et al. Dynamic contrast-enhanced CT in patients treated with sorafenib and erlotinib for non-small cell lung cancer: a new method of monitoring treatment? Eur Radiol 2010;20:2890-8.

16. Kiessling F, Boese J, Corvinus C, et al. Perfusion CT in patients with advanced bronchial carcinomas: a novel chance for characterization and treatment monitoring? Eur Radiol 2004;14:1226-33.

17. Valentin J. Avoidance of radiation injuries from medical interventional procedures. Annals of the ICRP 2000;30:7-67.

18. Stroian G, Martens C, Souhami L, Collins DL, Seuntjens J. Local correlation between monte-carlo dose and radiation-induced fibrosis in lung cancer patients. Int J Radiat Oncol Biol Phys 2008;70:921-30.

19. Hoang JK, Hoagland LF, Coleman RE, Coan AD, Herndon JE, 2nd, Patz EF, Jr. Prognostic value of fluorine-18 fluorodeoxyglucose positron emission tomography imaging in patients with advanced-stage non-small-cell lung carcinoma. Journal of clinical oncology : official journal of the American Society of Clinical Oncology 2008;26:1459-64.

20. Lazanyi KS, Abramyuk A, Wolf G, et al. Usefulness of dynamic contrast enhanced computed tomography in patients with non-small-cell lung cancer scheduled for radiation therapy. Lung Cancer 2010;70:280-5.

21. Donmez FY, Yekeler E, Saeidi V, Tunaci A, Tunaci M, Acunas G. Dynamic contrast enhancement patterns of solitary pulmonary nodules on 3D gradient-recalled echo MRI. AJR Am J Roentgenol 2007;189:1380-6.

22. Swensen SJ, Viggiano RW, Midthun DE, et al. Lung nodule enhancement at CT: multicenter study. Radiology 2000;214:73-80.

23. Yamashita K, Matsunobe S, Tsuda T, et al. Solitary pulmonary nodule: preliminary study of evaluation with incremental dynamic CT. Radiology 1995;194:399-405.

24. Wang J, Wu N, Cham MD, Song Y. Tumor response in patients with advanced non-small cell lung cancer: perfusion CT evaluation of chemotherapy and radiation therapy. AJR American journal of roentgenology 2009;193:1090-6.

25. Patz EF, Jr., Connolly J, Herndon J. Prognostic value of thoracic FDG PET imaging after treatment for non-small cell lung cancer. AJR American journal of roentgenology 2000;174:769-74.

26. Decoster L, Schallier D, Everaert H, et al. Complete metabolic tumour response, assessed by 18-fluorodeoxyglucose positron emission tomography (18FDG-PET), after induction chemotherapy predicts a favourable outcome in patients with locally advanced non-small cell lung cancer (NSCLC). Lung cancer 2008;62:55-61.

27. Woodford C, Yartsev S, Dar AR, Bauman G, Van Dyk J. Adaptive radiotherapy planning on decreasing gross tumor volumes as seen on megavoltage computed tomography images. International journal of radiation oncology, biology, physics 2007;69:1316-22.

28. Werner-Wasik M, Xiao Y, Pequignot E, Curran WJ, Hauck W. Assessment of lung cancer response after nonoperative therapy: tumor diameter, bidimensional product, and volume. A serial CT scan-based study. International journal of radiation oncology, biology, physics 2001;51:56-61.

ABSTRACT (IN KOREAN)

진행성 폐암 환자에서 항암 화학 치료 또는 방사선 치료 후 역동적 조영 증강 CT를 이용한 치료 반응 평가에 대한 연구

<지도교수 김 태 훈>

연세대학교 대학원 의학과

유 미 리

1. **목적:** 진행성 폐암 환자에서 초기 치료 후 Dynamic contrast-enhanced CT (이하 DCE-CT) 를 이용한 조영 증강 양상으로 항암치료 반응을 예측할 수 있는지 알고자 했다
2. **대상과 방법:** 진행성 폐암 환자에서 화학요법 및 방사선 치료 후 DCE-CT 를 시행한 사람을 대상으로 두 개의 연구 집단을 만들었다. 그룹 A 에서는 치료 후 DCE-CT 와 PET-CT 를 시행한 65 명의 환자를 대상으로 최고 표준 섭취값 (이하 SUVmax) 2.5 를 기준으로 두 그룹 (불완전 반응과 완전 반응 그룹)으로 나누었고, 그룹 B 에서는 DCE-CT 와 추적 CT 를 시행한 환자 42 명을 대상으로 추적 CT 에서 RECIST 1.1 에 따라 세 그룹으로 나누었다. DCE-CT 는 조영제 주입 전과 주입 30, 60, 90, 120 초와 5 분 후에 시행했다. 우리는 DCE-CT 에서 최고, 전체 조영 증강 (이하 PE, NE), 상대 증강 비 (이하 RER), 세척값 (이하 WO), 그리고 시간-음영곡선 (이하 TDC) (A, B, C, D 형)을 평가했다.
3. **결과:** PE와 NE는 불완전 반응 그룹 (이하 NR)에서 완전 반응 그룹(이하 CR)보다 유의하게 높았다 ($p < 0.05$). NR 그룹은 DCE-CT에서 가파른 가속 기울기를 가진 급속 조영 증강을 보이는 반면 CR 그룹은 느린 조영 증강을 보였다. 120초까지의 RER 역시 PET-CT 상 SUVmax와 중간 정도의 연관 관계를 보였다 ($r = 0.373$ to 0.603, $p < 0.01$).

   NE 와 PE 값은 진행성 질환 (이하 PD)그룹에서 안정성 질환 (이하 SD)이나

부분 관해 (이하 PR) 그룹보다 유의하게 높았다 ($p < 0.05$). B, C, 그리고 D TDC 타입은 대부분 PR 과 SD 그룹에서 관찰된 반면 (96.0%), 빠른 wash-in과 washout을 보이는 A형은 SD와 PD그룹에서 대부분 관찰되었으며 (97.2%), 이들 SD와 PD그룹간에는 PE와 NE가 유의한 차이가 있었다.

4. **결론:** DCE-CT 서 조영 증강 양상은 치료 결과에 따라 유의하게 달랐다. 그러므로 DCE-CT 는 진행성 폐암에서 치료 반응을 예측하는데 도움이 된다.

핵심되는 말: 폐암, 역동적 전산화 단층 촬영, 치료 감시